



Fragments in Bromodomain Drug Discovery

Journal:	<i>MedChemComm</i>
Manuscript ID:	MD-REV-05-2015-000209.R1
Article Type:	Review Article
Date Submitted by the Author:	30-Jun-2015
Complete List of Authors:	Bamborough, P; GlaxoSmithKline, Chung, Chun-wa; GlaxoSmithKline, Computational and Structural Chemistry

Cite this: DOI: 10.1039/c0xx00000x

www.rsc.org/xxxxxx

ARTICLE TYPE

Fragments in Bromodomain Drug Discovery

Paul Bamborough^{*a} and Chun-wa Chung^a

Received (in XXX, XXX) Xth XXXXXXXXX 20XX, Accepted Xth XXXXXXXXX 20XX

DOI: 10.1039/b000000x

5 Fragment-based approaches have been successfully applied to the discovery and optimisation of ligands for a wide range of targets. These concepts are proving valuable for bromodomain-containing proteins, an emerging family of epigenetic regulators. This review gives examples in which fragment-based drug discovery concepts are helping to find and optimise bromodomain inhibitors, with early successes against the BET subfamily now extending to other members of the target class.

10 Introduction

Following the discovery that small-molecule binding to the acetyl-lysine (KAc) pocket of bromodomain modules can block the recognition of their acetylated partner proteins, bromodomains have become a very active target class for drug discovery. Excitement has been fuelled by their potential tractability and the prospect of finding novel epigenetic mechanisms to tackle complex diseases such as cancer and inflammation. Inhibitors of the BET (Bromodomain and Extra Terminal domain) family of tandem bromodomain-containing proteins (BRD2, BRD3, BRD4 and BRDT) exhibit wide-ranging biological effects and therapeutic potential.^{1,2} Indeed, the first BET inhibitors (including 1-4, Figure 1) were identified through their effects in cellular systems.³⁻⁶ For example, 1 was found in an ApoA1 upregulator reporter assay while seeking leads for atherosclerosis. The application of chemoproteomics, biophysics and crystallography proved that its mode of action was histone-competitive bromodomain binding.^{3,4} X-ray crystallography has revealed the detailed interactions of these and other inhibitors with bromodomain acetyl-lysine sites, providing a compelling rationale to pursue this domain class through target-based lead discovery and optimisation approaches. The breadth of published bromodomain inhibitors, especially those for the BET family, has been comprehensively reviewed elsewhere.^{7,8} In this article we will concentrate on case histories using fragment approaches, addressing questions relevant to fragment-based drug discovery within this target class of related proteins. These include the opportunities of targeting a conserved site, the advantages from transferring chemical knowledge between targets, and the challenges of achieving selectivity and chemical novelty.

40 Bromodomain structure, acetyl-lysine recognition and mimicry

At least 42 human genes contain one or more bromodomains, modules whose function is to bind appropriately lysine-acetylated modified forms of their targets (Figure 2). Although other interacting proteins have been reported, histone tails are the most commonly known binding partners. In this context, the role of

bromodomain modules is thought to be to recruit additional effectors to sites of histone acetylation around activated genes, so acting as readers of the “histone code”.⁹⁻¹²

50 Bromodomains form four-helical bundles, with the peptide-binding site located at the end furthest from the two termini (Figure 3). Most bromodomains recognise their targets by means of multiple interactions within and outside their acetyl-lysine sites. The acetylated lysine itself is bound by a cluster of conserved residues, in particular an asparagine and tyrosine structural motif, and associated conserved water molecules (Figure 3). In contrast to these “typical” bromodomains, some lack these conserved residues (Figure 2), and it is unclear whether they still bind to acetylated lysine peptides, have alternative substrate recognition specificity, or are “pseudo-bromodomains” without binding competency.

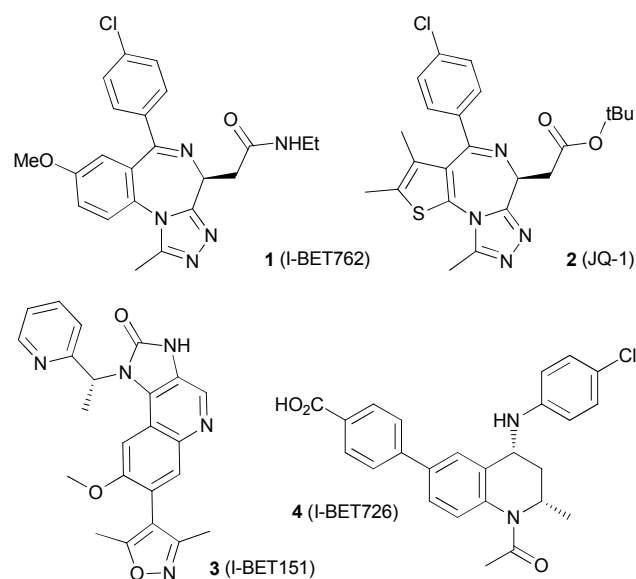


Fig. 1 Some BET inhibitors discovered directly or indirectly through cell-based screening.

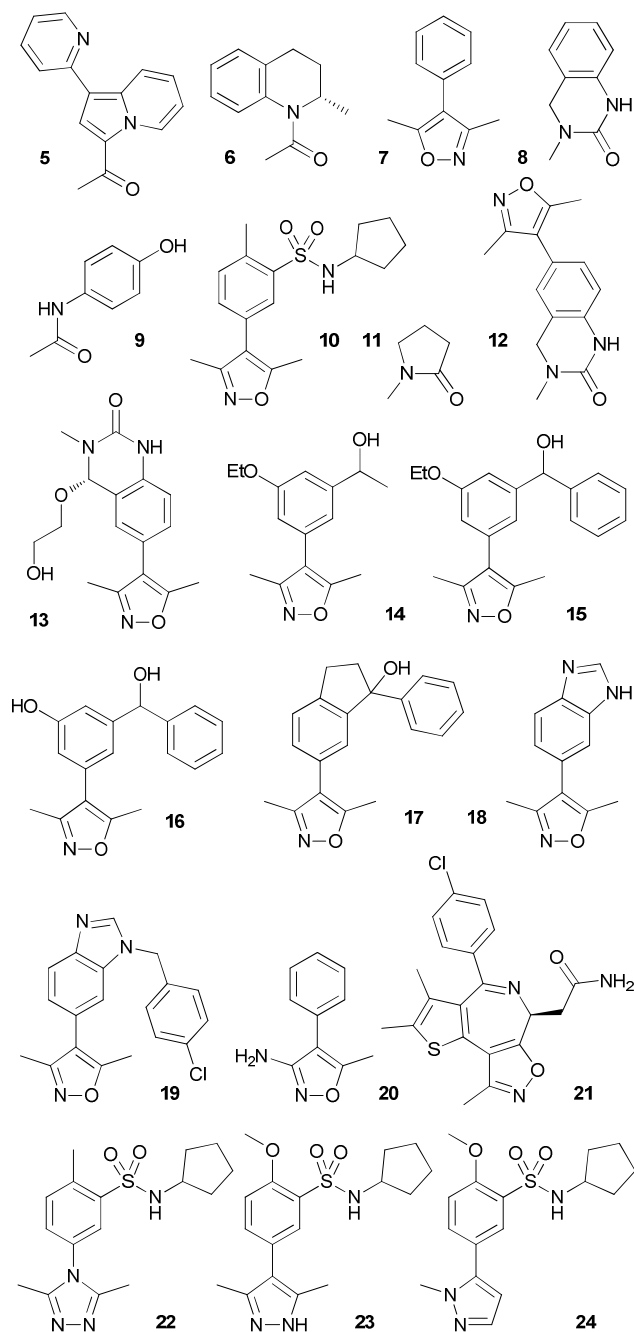


Fig. 4 Some BET bromodomain fragments and elaborated inhibitors

In one example, information from historical work on BET bromodomain inhibitors was used to assemble a knowledge-based fragment library.²⁶ This was screened against three BET family bromodomains in competition-binding fluorescence anisotropy assays. From this, crystal structures of multiple hits bound to the KAc-site of BRD2 BD1 were solved. With reference to the interactions made by acetyl-lysine shown in Figure 3, for almost all fragments the indirect W1-water mediated hydrogen bond to tyrosine Y113 was shorter than the direct hydrogen bond to the conserved asparagine N156, suggesting that this is the stronger interaction.

Four of the hits (5-8) are shown in Figure 4.^{26,27} Although

15 originating from BET family bromodomain screens, several of these fragments illustrate the ability of fragments to bind to the KAc-site of more than one bromodomain. The indolizine (5) is a micromolar-affinity BET fragment, which uses its ketone group as an acetyl-lysine mimetic, and which was also optimised against the BAZ2A/B bromodomains (see the BAZ2A/B section below). The BRD2 BD1-bound crystal structure of 5 prompted the crystallographic screening of acetaminophen (9), which although too weak to detect in the binding assays was found to bind to the acetyl-lysine site of BRD2 BD1 in the same manner as 5. The K_d of 9 for BRD4 BD1 has been determined to be of the order of 250-290 μM using a sensitive ^{19}F protein NMR approach in which fluoro-tyrosine and fluoro-tryptophan labels were incorporated into the region of the KAc-site.²⁸ 9 binds to the bromodomain of CREBBP and to that of BAZ2B in a near-identical way, which will be a recurring theme in this review.^{26,29}

Another example of cross-bromodomain fragment binding is provided by the tetrahydroquinoline (THQ) 6. Its racemate was originally detected in a fragment screen carried out against CREBBP (see the CREBBP section below).³⁰ Independently, inhibitors containing the THQ fragment 6 were found as ApoA1 upregulators using a diversity screen in a cellular reporter assay. Optimisation of these for atherosclerosis led directly to 4 (I-BET726). Only later, as similar discoveries were made for other compound classes, was it recognised that the BET family bromodomains were the molecular targets of this series, and crystal structures solved confirming its binding to the bromodomain of BRD2 BD1.^{5,26} This fragment provides the first of several interesting examples of the discovery of similar bromodomain inhibitor fragments by parallel, independent strategies. Another instance of this is the range of inhibitors based on the dimethyl isoxazole fragment 7, which most likely features within the compound collections of numerous organizations because of the availability of (3,5-dimethylisoxazol-4-yl)boronic acid as a commercial reagent.

50 Fragment-based discovery and optimisation of dimethyl isoxazoles.

At least three groups have reported the independent discovery and optimisation of the phenyl dimethylisoxazole fragment 7 or close analogues. In our case, as described above for the tetrahydroquinoline 6, the dimethyl isoxazole motif was found through a reporter assay, and optimised to 3 (I-BET151) using cellular SAR.^{31,32} Subsequently a crystal structure of BRD2 BD1 bound to 7 was used as the starting point for a proof-of-concept fragment optimisation study, aimed at generating a submicromolar BET bromodomain compound with cellular activity through structure-based fragment optimisation.²⁷ Structure-activity relationships from previous optimisation of multiple series suggested a viable fragment optimisation strategy. It was apparent that structurally diverse compounds such as 1-4 fill the KAc-site, but also project aromatic substituents outwards onto a lipophilic region termed the WPF shelf (Figure 3C).^{1-3,5,31} This suggested that growing from a KAc-site fragment to make lipophilic interactions with the WPF shelf could provide significant boosts in activity.

Cite this: DOI: 10.1039/c0xx00000x

www.rsc.org/xxxxxx

ARTICLE TYPE

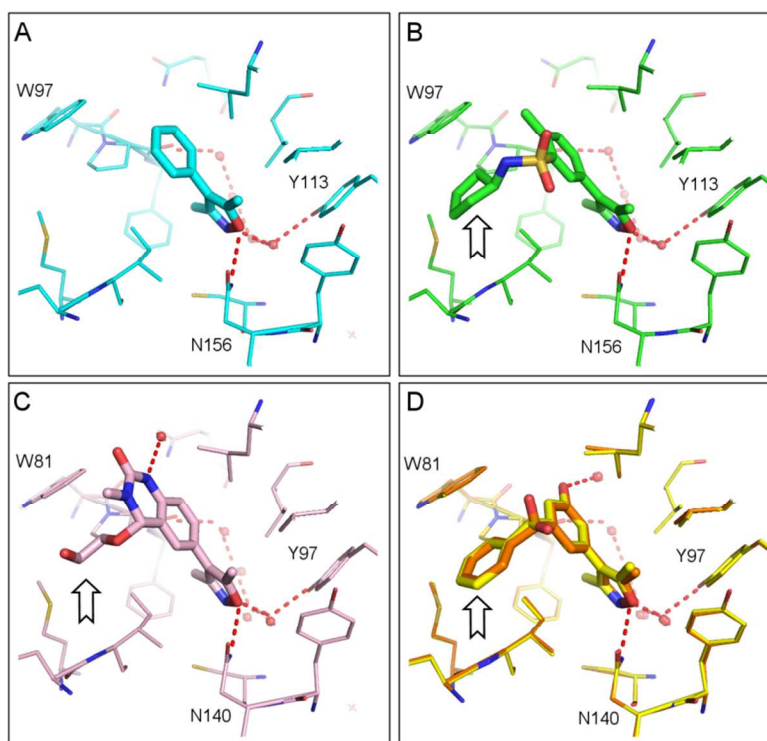


Fig. 5 Crystal structures of BRD2 BD1 bound to A) **7** (cyan, PDB: 4alh) and B) optimised analogue **10** (green, PDB: 4a9m). Crystal structures of BRD4 BD1 bound to C) **13** (pink, PDB: 3svf), D) (*R*)- and (*S*)- compound **16** (PDB: 4j0r, yellow; 4j0s, orange). Black arrows mark the WPF shelf.

To apply this to the isoxazole series, a 3D pharmacophore was used to search for compounds able to satisfy the WPF shelf interaction. This identified hits such as **10**, a sub-micromolar BET inhibitor with activity against a known BET-driven phenotype, the production of inflammatory cytokines.²⁷ The cyclopentyl sulfonamide substituent (Figure 5A,B) contributed over 100-fold improvement in binding affinity. Little medicinal chemistry resource was required to get to this point, since many key compounds were commercially available, showing that the BET family bromodomains are highly tractable both to fragment screening and optimisation.

An independent and extensive exploration of the dimethyl isoxazole fragment began with the observation that **11** (the solvent *N*-methyl pyrrolidine or NMP) binds in the KAc-sites of several bromodomains.³³ Following a hypothesis that other *N*-methyl lactams and related compounds could bind in a similar way, the *N*-methyl dihydroquinazolinone **12** was tested and found active in a BRD4 AlphaScreen peptide displacement assay.³⁴ However, when the BRD4 BD1 X-ray complex with **12** was solved, it was discovered that the dihydroquinazolinone ring had oxidised and that ethylene glycol from the buffer had added to the iminium intermediate, giving **13**. Unexpectedly, **13** bound in the KAc pocket using its dimethyl isoxazole as the acetyl-lysine mimic rather than its dihydroquinazolinone. Its hydroxyethyl

group occupied the WPF shelf (Figure 5C). This prompted further analogue screening and led to the discovery of **14** as a BET KAc-site binding fragment structurally unrelated to the starting point. The (*R*)-enantiomer of **14** crystallised preferentially with BRD4 BD1. The discovery that **14** showed comparable inhibition of CREBBP triggered further work against that bromodomain (see the CREBBP section below).

A fragment-growing approach was then used to optimise the interactions of **14** with BRD4, and to increase selectivity over CREBBP. Initially, the WPF shelf of BRD4 BD1 was targeted, using the pendant phenyl ring of compound **15**, maintaining ligand efficiency and leading to a 7.5-fold improvement in potency relative to **14**. A second iteration targeted water molecules of the ZA channel region of the binding site, producing improved potency in the form of compound **16** (Figure 5D). Both (*R*)- and (*S*)-enantiomers had similar BET binding activity, and submicromolar activity in an acute myeloid leukemia cell line.

Follow-up work concentrated on derivatisation of the phenyl ring.³⁵ Rigidification of the benzylic substituent led to **17**. When co-crystallised, the (*R*)-enantiomer was found to bind to BRD4 BD1, with the phenyl ring occupying the WPF shelf. However, due to chemical instability of this series efforts were concentrated on other bicyclic templates such as the benzimidazole **18**. Compound **19** was one example which showed an increased

window of selectivity over CREBBP.³⁵

A third group has also described the independent discovery of **20**, a fragment closely related to **7**.³⁶ They chose to use this information indirectly, identifying an opportunity for isosteric ring replacement within an existing BET inhibitor, the triazolodiazepine **2**.² Comparison of the bound X-ray structures showed that the triazole moiety of **2** could be replaced by the isoxazole, resulting in the isoxazole azepine **21**.

Other molecules containing the dimethyl isoxazole fragment have featured in several more BET publications and patents. One recent extension was a systematic exploration of alternative KAc-mimetics to the isoxazole.³⁷ Taking **10** as a starting point, heterocyclic replacements were synthesised and evaluated in BET AlphaScreen assays, as well as for microsomal stability. While none improved on the potency of the isoxazole, several were active. Surprisingly, given the presence of this substructure in potent BET inhibitors such as **1** and **2**, the triazole **22** was much weaker than the pyrazoles **23** and **24**, with barely detectable activity at 5 μM compound concentration, compared to the BRD4 BD1 IC₅₀ of 0.67 μM for **10**.

The crystallographic binding modes of **16** and **10** in BRD4 BD1 and BRD2 BD1 respectively are very similar (Figure 5). Both molecules reach similar potencies and ligand efficiencies, albeit measured in different assays, but are chemically distinct, an interesting outcome given that the same fragment provided the starting point for each. Other independent groups working on the same fragment also arrived at comparable but different optimised compounds. It might be thought that targeting a particular binding site with knowledge-based fragment libraries constructed using the same information could lead different investigators down parallel tracks to the same end-point. These examples show that for BET bromodomains this has not been the case. It seems that chemical novelty as well as selectivity and potency is quite achievable using FBDD for the BET bromodomains.

Dihydroquinazolinone fragment optimisation

As explained above, the acetyl-lysine mimetic of fragment **12** was not the intended *N*-methyl dihydroquinazolinone.³⁴ Even so, this bicyclic system is a competent acetyl-lysine mimic. Optimisation of the simple bromide analogue **25** (Figure 6) produced the potent and selective BET bromodomain chemical probe PFI-1 (**26**).³⁸ As with the optimisation of **7** to produce **10** and **16**, this was achieved by growing from the acetyl-lysine site fragment using a linked lipophilic group targeting the WPF shelf (Figure 7). Again, the conformational preference of the linker was critical, but because the WPF shelf was approached from a different starting point the structure-activity relationships differed between the two series. For example, in the dimethyl isoxazole sulfonamide series, alkyl groups such as the cyclopentyl of **10** were preferred over aryl rings, whereas aryl rings were superior in the dihydroquinazolinone series. In addition, the sulfonamide of the reversed directionality was preferred, such that **27** was significantly less potent than **26**.³⁸

In light of the instability to oxidative insertion that gave rise to **13** from **12**, the quinolinone **28** was made. This aromatised analogue of the dihydroquinazolinone **26** had similar potency and selectivity. Through crystallography, the pendant WPF-shelf methoxyphenyl was identified as a suitable place for further

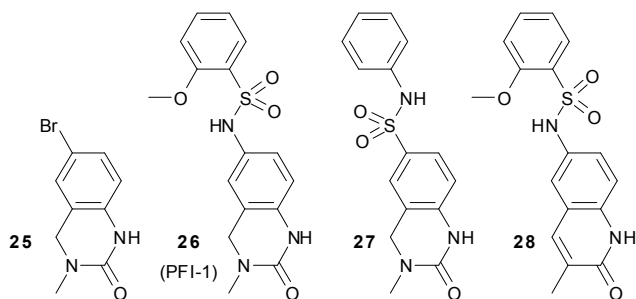


Fig. 6 Dihydroquinazolinones and related BET compounds **25-28**

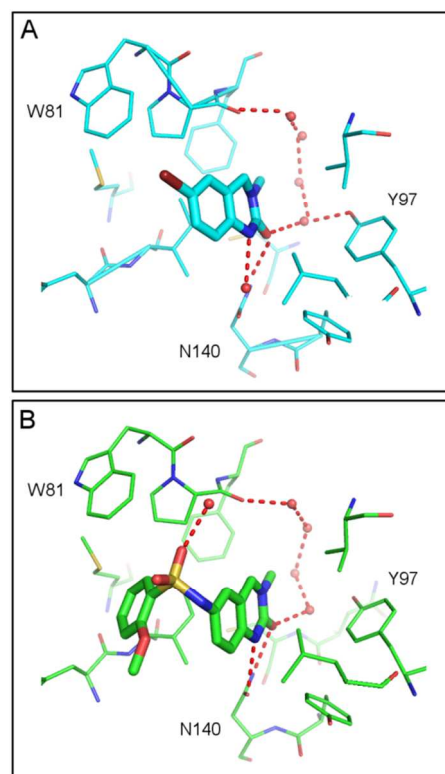


Fig. 7 Crystal structures of BRD4 BD1 bound to A) compound **25** (PDB: 4hbv) and B) optimised compound **26** (PDB: 4e96).

derivatisation. When the methoxy position of **28** was substituted with a linker connected to a biotin group, this provided an effective affinity-capture tool for chemoproteomic studies.³⁹

BET X-ray screening, and 2-thiazolidinones

In these examples of BET bromodomain fragment screening, most groups chose to take advantage of prior X-ray structural knowledge to bias the screening library towards groups thought likely to be active. Fragments containing features important for binding to the acetyl-lysine site (the conserved hydrogen bonding functionalities and the small lipophilic methyl group of the acetyl moiety) were used to populate targeted libraries. These were then screened using either direct-binding methods such as NMR, or competition binding assays using labelled peptides or small molecules. Once they were known to bind, X-ray crystallography was used to elucidate the binding modes to support optimisation.

Crystallography can also be used as a low-throughput, high-

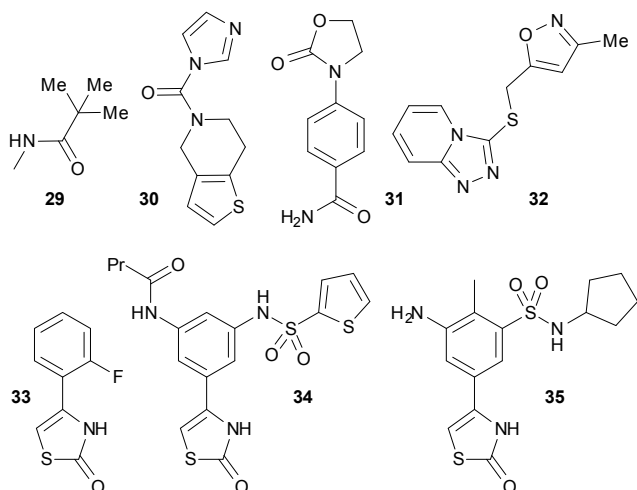


Fig. 8 BRD4 X-ray screening hits **29-33** and optimised molecules **34-35**

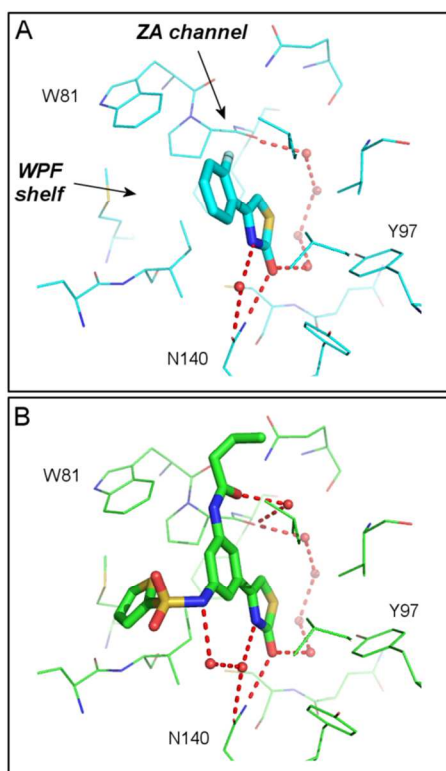


Fig. 9 Crystal structures of BRD4 BD1 bound to A) compound **33** (PDB: 4hxn) and B) compound **34** (PDB: 4hxm).

sensitivity screening assay, albeit one that does not quantify affinity or ligand efficiency.^{40,41} This approach has been applied to the BET family bromodomains. For example, X-ray screening was used to find and determine the binding mode of three very small fragments in BRD4 BD1, such as **29** (Figure 8).⁴²

Optimisation of BET bromodomain fragments discovered through crystallographic screening has been reported in one instance.⁴³ As with many other bromodomain fragment screens, this made use of a knowledge-based library, selected using computational docking of diverse fragments against BRD4 BD1. Docked poses were checked for interactions with the conserved

asparagine Asn140, and a limited number were tested directly by crystallography without any intervening screen. Out of these, ~25% were observed to bind in the KAc-site (e.g. **30-33**, Figure 8). The thiazolidinone **33** was chosen for optimisation against BRD4 BD1, exploring a number of different substituent positions targeting specific regions of the protein (Figure 9).⁴³ As with the optimisation that led to compound **26**, aryl sulfonamides at the 3-position were found to be optimal for targeting the WPF shelf. Separately, position 5 was elaborated to grow into the ZA channel. Both substituents were then combined, giving micromolar compounds such as **34** (Figure 9) which had some antiproliferative activity in a colon cancer cell line. A follow-up publication described the reversal of the 3-sulfonamide linker.⁴⁴ In this case, pendant cycloalkyl sulfonamides were preferred to aromatic, although intriguingly these do not appear to occupy the WPF shelf. The 5-substituent could be shortened, as for example in **35**, maintaining BRD4 BD1 binding and improving cellular potency.

PCAF (KAT2B)

The first fragment screen against a bromodomain was performed not against a BET subfamily member, but against PCAF (P300/CBP-associated factor, also known as KAT2B; figure 2).⁴⁰ ¹⁵N NMR was highly influential in this work. First, it was used to solve the solution structure of the PCAF bromodomain, then to screen compound libraries for small molecule binding partners.^{45,46} Shifts in the assigned protein backbone NMR resonances showed that the compounds interact with PCAF in the same region as the acetyl-lysine peptide binding site. The potency of one of the hits, fragment **36** (Figure 10; estimated IC₅₀ of 5 μM) was improved to 1.6 μM in compound **37**. While no obvious acetyl-lysine mimic exists in these compounds, and a crystal structure has yet to be reported, a binding model was produced with the help of restraints from the NMR data. Analogues were active in a reporter assay measuring HIV-1 LTR-luciferase expression,⁴⁷ and inhibition of HIV infection in a T-cell line has been reported for members of the series.⁴⁸

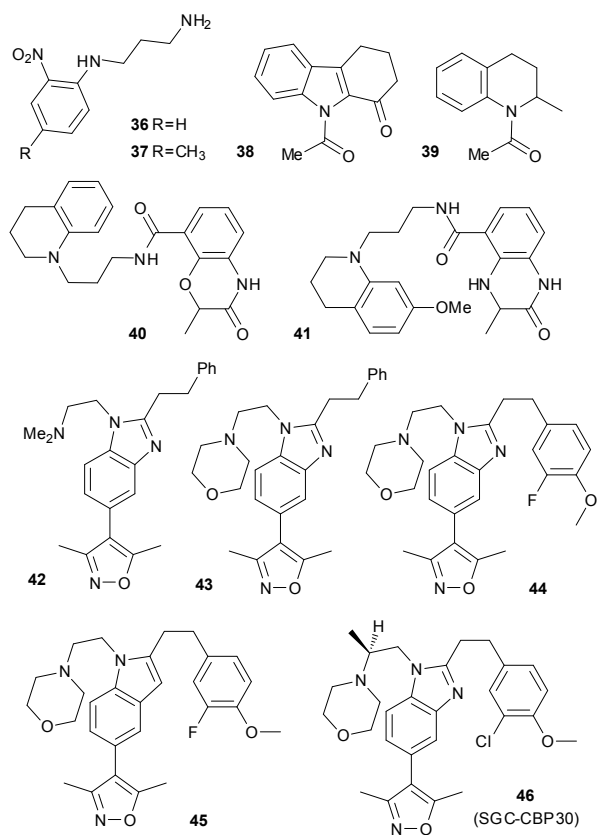


Fig. 10 PCAF fragments **36-37** and CREBBP fragments **38-46**

CREBBP

Following the successful screen against PCAF above, the same laboratory applied a similar approach to the bromodomain of CREBBP (cAMP Response Element-Binding protein Binding Protein).³⁰ In this case, protein NMR screening was performed against a pooled library of fragments chosen to mimic the acetyl-lysine group. As in the PCAF case-study, fragments such as **38** and **39** (Figure 10) interact with CREBBP residues close to the acetyl-lysine site. Fragment **38** was estimated to have K_d of around 20 μM by tryptophan fluorescence. A particularly encouraging finding was that most of the CREBBP fragments did not bind to PCAF, suggesting that even such small compounds

can achieve some degree of discrimination between bromodomains. While optimisation of **39** against CREBBP has not been reported, its (*S*)-enantiomer **6** binds to other bromodomains, including BRD2 BD1, and forms the KAc-mimetic at the heart of a potent optimised series of BET inhibitors including **4** (see above).^{4,26}

In a further example of chemical cross-over between inhibitors of different bromodomains, optimisation against CREBBP of fragments first known as BET family KAc-site binders has been described. The dihydroquinazolinone fragments **8** and **12** (Figure 4) were crystallised in CREBBP. Modification to overcome oxidative instability (see above) led to the synthesis of benzoxazinone and dihydroquinoxalinone isosteres (**40** and **41**, Figure 10).⁴⁹ In this work, the amide substituents were chosen by an *in silico* screen targeting the ZA channel region of the CREBBP bromodomain. Unexpectedly, the two compounds have very different CREBBP AlphaScreen IC₅₀s, with the benzoxazinone **40** being relatively modest compared to **41** (51 μM vs 323 nM). The poor activity of **40** was rationalised by an unfavourable electrostatic interaction between the benzoxazinone ring oxygen and the backbone carbonyl of Pro1110. Another factor was the stabilisation of an undesired conformation via formation of an internal H-bond between the benzoxazinone oxygen and the amide NH group. When the crystal structure of (*R*)-**41** in CREBBP was solved, it was found that its tetrahydroquinoline substituent does not bind in the ZA channel. Instead, it occupies a CREBBP site roughly analogous to the WPF shelf of BET (Figure 11A). This pocket was not seen in previous crystal structures, being formed by movement of the mobile Arg1173 sidechain. A K_d of 390 nM for (*R*)-**41** was obtained for CREBBP by ITC, 3-4 fold lower than the K_d of 1.4 μM for BRD4 BD1.

Like the dihydroquinazolinone **25**, the isoxazole KAc-mimetic was originally found for BET (see above), and has also been optimised for CREBBP.⁵⁰ Starting from the unselective **18** (IC₅₀ ~4 μM vs CREBBP, ~6 μM vs BRD4 BD1), parallel synthesis was used to expand SAR at the benzimidazole 1- and 2-positions. Building blocks were chosen to target regions of the protein analogous to the BET WPF shelf and ZA channel, but additional diversity was also included. Compound **42** showed increased CREBBP potency (AlphaScreen IC₅₀ ~500 μM) and

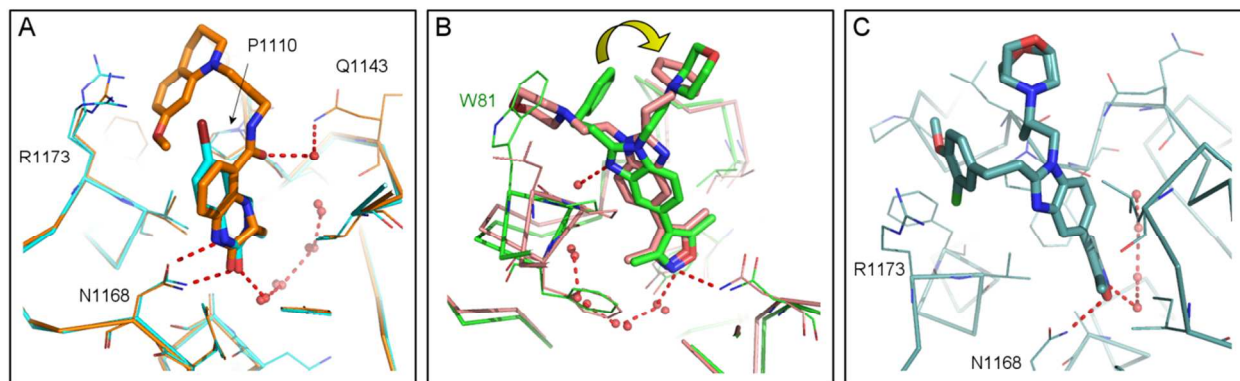


Fig11 A) Crystal structure of CREBBP bound to **25** (cyan, PDB: 4nyv) and **41** (orange, PDB: 4nyx). B) Crystal structures of **43** bound to BRD4 BD1 (green, PDB: 4nr8) and CREBBP (pink, PDB: 4nr5). The yellow arrow highlights the movement of the C2-linked phenethyl ring between the two structures. C) Crystal structure of CREBBP bound to **46**, with the morpholine modelled in two conformations (PDB: 4nr7).

Cite this: DOI: 10.1039/c0xx00000x

www.rsc.org/xxxxxx

ARTICLE TYPE

little effect on BRD4 BD1 as assessed by stabilisation of thermal melting.

Optimisation of the benzimidazole N-1 amine substituent led to the morpholine **43**, which had CREBBP IC_{50} ~160 μ M. This was crystallised in CREBBP and BRD4 BD1. A 180° rotation around the isoxazole-benzimidazole bond leads to a different binding orientation in each bromodomain (Figure 11B), with each substituent occupying a different pocket. Although the C2-linked phenethyl substituent bound on a rather exposed hydrophobic surface patch in each bromodomain, diverse analogues were made to vary the terminal ring. This led to compounds such as **44**, whose K_d for CREBBP was measured to be 22 nM by isothermal titration calorimetry, with 20-fold selectivity over BRD4 BD1.

The crystal structure of **43** in BRD4 BD1 also revealed the presence of a hydrogen-bond between the benzimidazole N-3 atom and a water molecule that was not seen in CREBBP (Figure 11B). This observation led to the synthesis of the indole analogue **45**.⁵⁰ The prediction that this compound should be less active against BRD4 BD1 was confirmed by thermal melting. However, it showed surprisingly little thermal stabilisation of CREBBP either, despite the lack of visible interactions made by the benzimidazole N-3 nitrogen of **43**. The X-ray structures also showed that the C-2 ethyl linker made hydrophobic contacts with the BRD4 BD1 WPF motif tryptophan, Trp81, and that in CREBBP the linker was more exposed (Figure 11B). As a result, polar and sterically constrained C-2 linkers were prepared, but neither of these led to an improvement. However, a similar conformational constraint approach at the N-1 linker gave better results, the chiral compound **46** being twice as potent against CREBBP than **45** (K_d 21 nM). Crystallography revealed that the chloro-methoxy-phenyl ring of **46** binds in a similar place to the methoxyphenyl of **41**, in the binding site produced by movement of the sidechain of Arg1173 (Figure 11C). **46** (SGC-CBP30) appears to be selective for CREBBP and its closest homologue EP300 over other bromodomains, including 40-fold (by ITC) over the BET family. This is another example of the use of structure-based design to generate selectivity from an unselective fragment starting point.

BAZ2A and BAZ2B

Unbiased or diverse fragment libraries have been employed less frequently than targeted libraries in published bromodomain fragment screens. In one example, a diverse fragment set was screened in a high-concentration AlphaScreen peptide competition format against BRD4 BD1, CREBBP, and also a bromodomain with lower predicted ligandability, that of BAZ2B (Bromodomain Adjacent to Zinc-finger domain 2B).⁵¹ The hit-rates against the three bromodomains were reported to be consistent with their predicted druggability. As this assay format is known for its high false-positive rate, ligand-observed NMR was used to authenticate BAZ2B fragment binding, before the successful crystallisation of three fragment-bound X-ray

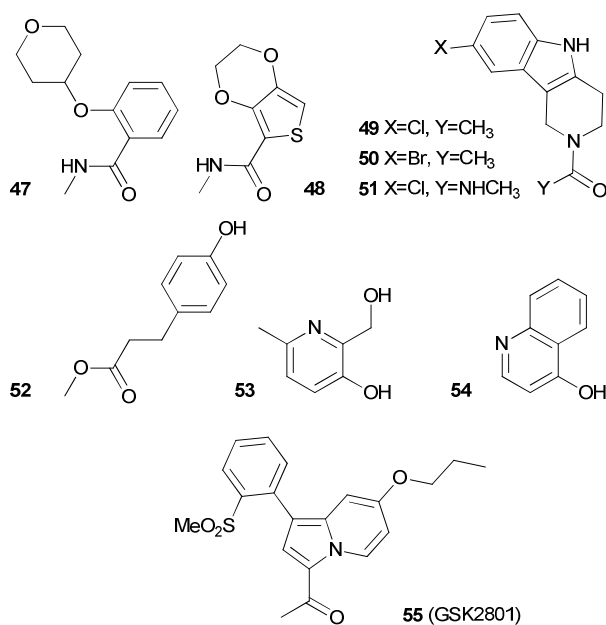


Fig. 12 BAZ2B fragments and optimised molecules 47-55

complexes (**47-49**, Figure 12). Analogues of fragment **49** were synthesised and tested, but large potency gains proved difficult to realise. In fact, the biggest improvements (less than threefold) came from the close analogues **50** and **51**. Interestingly, **50** but not **51** thermally stabilised CREBBP and both bromodomains of BRD2, providing another example of fragments binding to multiple bromodomains.

Crystal structures of BAZ2B complexed with other acetyl-lysine site binding fragments (e.g. **9** and **52-54**) have been released.²⁹ Their discovery story has not yet been published, but the binding mode of **9** in BAZ2B is identical to that in BRD2 BD1 and CREBBP, reinforcing the concept of common fragment starting points for multiple members of this target class.

55 (GSK2801) has been reported as a selective chemical probe for the bromodomains of BAZ2A and BAZ2B.⁵² By isothermal titration calorimetry, the compound has K_d of 136 nM and 257 nM for each bromodomain respectively. This molecule originated from optimisation of the BRD2 BD1 fragment **5** (Figure 4) against BAZ2A and BAZ2B. Selectivity over the BET bromodomains (e.g. BRD4 BD1 IC_{50} >50 μ M) was achieved with the help of the bulky *ortho*-sulfone substituent. This introduces a greater out-of-plane rotation to the indolizine-phenyl bond, leading to a molecule that is too wide to fit into the relatively narrow ZA channel in the BET bromodomains. The selectivity profile was supported by chemoproteomic profiling, in which an analogue of **55** immobilised on beads was used to pull down native bromodomain-containing proteins from cell lysate.⁵² Out of 18 proteins detected, only BAZ2A and BAZ2B showed dose-dependent competition with **55**. The compound was also active in a FRAP (Fluorescent Recovery After Photobleaching) assay with

transfected GFP-BAZ2A, accelerating recovery time to the same extent as an acetyl-lysine site mutated construct, providing direct evidence that the compound can engage intracellular BAZ2A. With favourable pharmacokinetic properties in mice, **55** was judged suitable for use as a cellular and *in vivo* chemical probe for BAZ2A/B bromodomain inhibition. Chemically distinct molecules identified through non-fragment approaches (e.g. BAZ2-ICR⁵³) provide opportunities to strengthen the BAZ2A/B-driven target interpretation of any phenotypes discovered.

10 ATAD2, and water network-displacing fragments.

Over-expression of ATAD2 (ATPase family, AAA domain containing 2), also known as ANCCA (AAA nuclear coregulator cancer-associated protein), is associated with poor outcomes in cancer.⁵⁴ Its bromodomain and that of its homologue ATAD2B are predicted to be among the least ligandable of all bromodomains.¹³ Consistent with this, reports of fragments that bind to the KAc-site of this protein have recently appeared, but so far all are relatively weak.

The first of these pointed out that screening of putative acetyl-lysine mimic fragments was hampered by the need to avoid DMSO as a solvent, since this is itself a competitive bromodomain binding fragment. X-ray screening of polar water-soluble fragments produced crystal structures of ATAD2 bound to fragments **56** and **57**, thymine (Figure 13).⁵⁵ X-ray soaking of analogues identified related nucleoside hits, including thymidine (**58**). ¹³C-methyl labelled HSQC NMR titrations were used to estimate K_d values of approximately 10 mM for **57** and **58**.

Another X-ray screen to identify ATAD2 inhibitors commented that the ATAD2 fragment screen had a relatively low hit-rate. It also found that known inhibitors of other bromodomains were relatively weak against ATAD2.⁵⁶ Despite this, the resulting dimethyl isoxazole hit **59** had K_d for ATAD2 of 200 μM (LE 0.28), comparable to that reported for the similar isoxazole fragments **7** and **14** to the BET bromodomain (see above).

These examples show that efficient fragment hits can be found, but so far only one example of optimisation has been reported.⁵⁷ Starting from the quinolinone fragment that acts as the acetyl-lysine mimetic of **28**, **60** was prepared as part of an array. Its dimethylamine group was chosen to target a cluster of acidic residues unique to ATAD2 (Asp1066, Asp1068 and Asp1071). An IC₅₀ of ~100 μM was found in a TR-FRET assay, and its specificity confirmed by ¹⁵N-¹H NMR. Optimisation of a more chemically tractable 1,7-naphthyridin-2(*1H*)-one template resulted in the first reported micromolar ATAD2 inhibitors (e.g. **61**, IC₅₀ 1.5 μM). Crystal structures (Figure 14) confirmed the role of the 1,7-naphthyridin-2(*1H*)-one as the acetyl-lysine mimetic and explained the improvement in potency afforded by the pyridyl substituent, which forms a direct hydrogen-bond with the backbone amide NH group of Asp1014 on the ZA loop.

The isomeric 1,5-naphthyridin-2(*1H*)-one **62** was also found independently by screening a pooled, unbiased fragment library by ¹H-¹⁵N SOFAST-HMQC NMR.⁵⁸ Other fragments binding in the ATAD2 KAc-site included **63-66**. After deconvolution, the same assay was used to determine the affinity of the hits, which had reasonably good ligand efficiency (K_d > ~600 μM, LE < ~0.38). Crystal structures of several hits were reported, mostly

showing typical interactions with the KAc-site pharmacophore, engaging the conserved asparagine Asn1064 and the W1 water associated with Tyr1021 in the expected manner. The benzimidazolone **64** is related to BET/BRPF1 fragment **73** which will be discussed later.

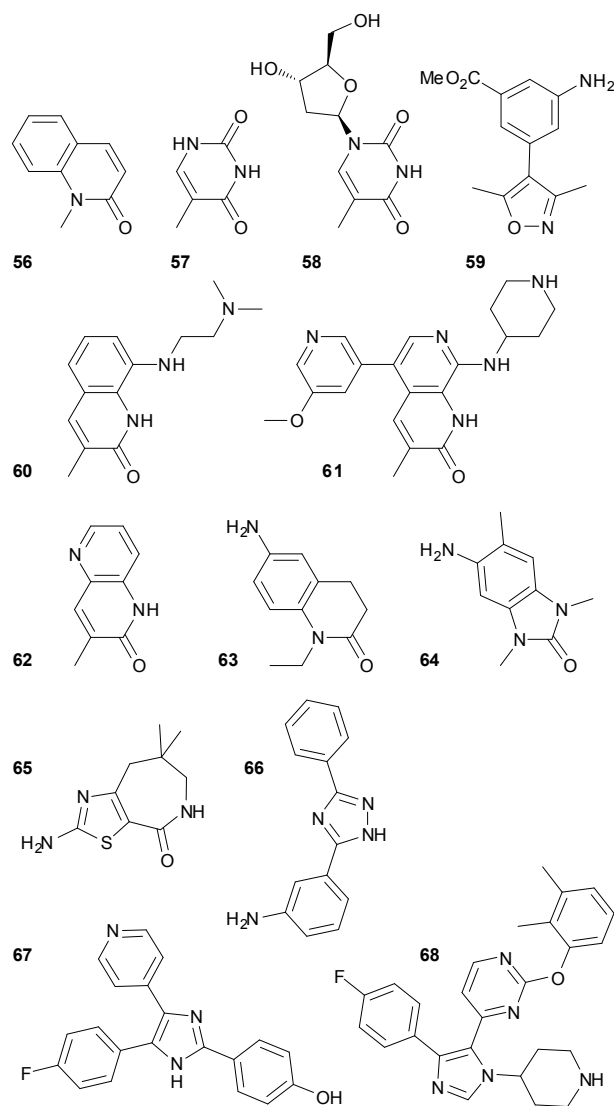


Fig. 13 ATAD2 fragments **56-66** and BRD4 BDI/p38 kinase inhibitors **67-68**.

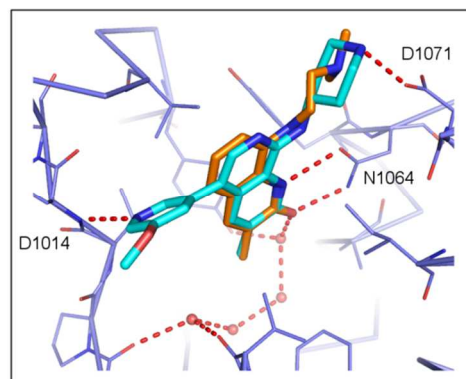


Fig. 14 X-ray structures of ATAD2 with **60** (orange, PDB:5a5p) and **61** (blue, PDB:5a5r).

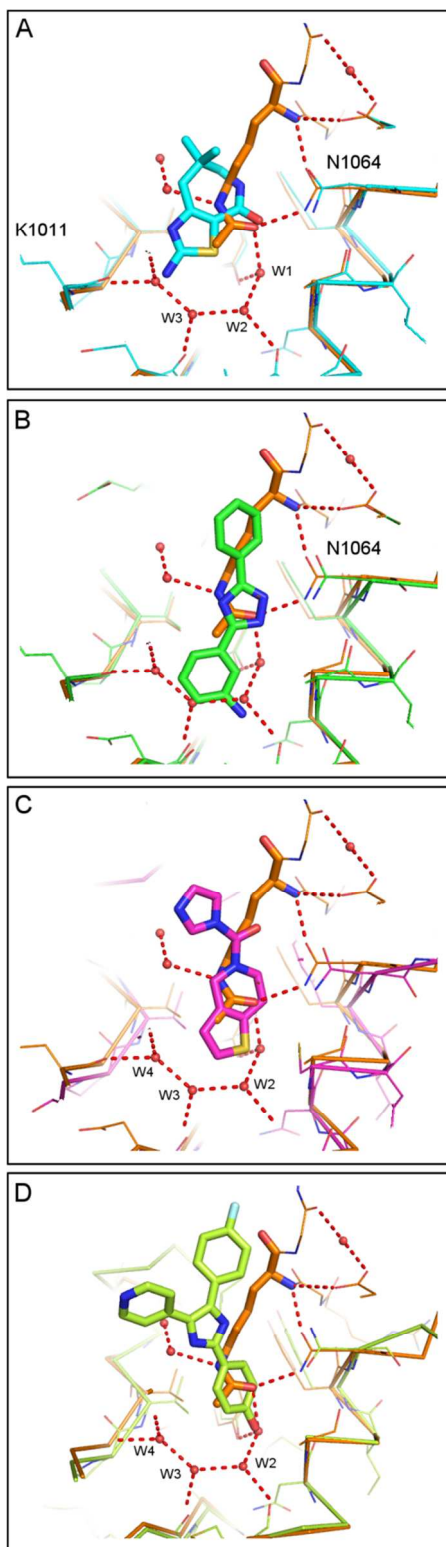


Fig. 15 Crystal structures of ATAD2 bound to H4K5Ac peptide (orange, PDB: 4quu) superimposed on A) ATAD2/**65** (cyan, PDB:4tz8); B) ATAD2/**66** (green, PDB: 4tz2); C) BRD4 BD1/**30** (magenta, PDB: 4hvk); D) BRD4 BD1/**67** (lime green, PDB: 4o77). Water molecules and H-bonds are shown for histone peptide complex (4quu). Water molecules remaining in the fragment complexes are labelled W1-W4.

Interestingly, two fragments (**65** and **66**) were found to exhibit novel binding modes. With only a few exceptions, known

10 bromodomain ligands bind with the conserved KAc-site network of four water molecules intact (W1-W4, Figure 3). Although **65** and **66** both still bind within the KAc-site, they were among the first fragments reported to displace some of the conserved water molecules. The lactam of fragment **65** (Kd 500 μ M, LE 0.33) 15 hydrogen-bonds to the conserved asparagine Asn1064 and to the W1 water as usual (Figure 15A). The thiazole sulfur binds in the acetyl-lysine methyl site. However, the fourth water of the network (W4) is displaced by the amine of **65**, which replaces the hydrogen bonds it normally makes with W3 and the carbonyl of 20 Lys1011.

Fragment **66** makes even more disruptive changes to the water network (Figure 15B). The triazole ring forms a direct hydrogen bond to Asn1064, but this large aromatic molecule goes even deeper, displacing all four conserved water molecules. Its aniline 25 group satisfies the hydrogen-bond normally made by the third water to the carbonyl of Ile1056. As **66** was among the least efficient of the hits reported in this study (Kd 600 μ M, LE 0.27), removal of the four water molecules of the conserved network may be energetically penalised. Until this point, these had been 30 present in almost all published experimental bromodomain crystal structures. It is possible that the water molecules of ATAD2 may be unusually weakly bound. If so, it is unclear whether this is a quirk of this particular truncated construct of the ATAD2 bromodomain, or is a feature of the full-length protein 35 and therefore pharmaceutically relevant. Further studies will be needed to explore these possibilities.

Alternatively, it is interesting to speculate that similar water displacement might be possible in other bromodomains. Indeed, displacement of one water molecule was seen in the binding of a 40 tetrahydrothieno[3,2-*c*]pyridine fragment **30** (Figure 8) to BRD4 BD1 (Figure 15C).⁴³ In this case, only weak activity was measured by fluorescence anisotropy (11% at 100 μ M) compared to other fragments from the same study such as **33** (43%). Several full-sized literature kinase inhibitors (e.g. the p38 inhibitors **67**, 45 SB-202190, and **68**, SB-284847-BT) also bind to the BRD4 BD1 bromodomain with modest potency (AlphaScreen IC₅₀ 2.5 μ M, LE \approx 0.31) by displacing some or all of the water network (Figure 15D).⁵⁹ Another example of complete displacement of water by a fragment is seen in the crystal structure of salicylic acid **69** bound 50 to the KAc-site of PB1 BD5, which will be discussed below in the PB1 section.

PB1

PB1 (Polybromodomain-containing protein 1) contains six bromodomains, with the fifth (BD5) predicted to be the most 55 tractable to small molecule inhibition.¹³ To date, there has been no reported chemistry targeting this protein. A crystal structure has been deposited in the protein databank of BD5 in complex with salicylic acid (**69**, Figure 16).⁶⁰ This fragment binds deep within the KAc-site, displacing all of the conserved water 60 molecules, in a similar position to the aniline moiety of **66** in ATAD2. PB1 BD5 crystal structures in complex with larger inhibitors structurally related to this fragment (**70**, **71**) have also been deposited.⁶⁰ It may be significant that these resemble PFI-3 (**72**), reportedly a dual inhibitor of the PB1 BD5 and SMARCA4 65 bromodomains (Kd 48 nM and 89 nM by ITC, respectively).⁶¹

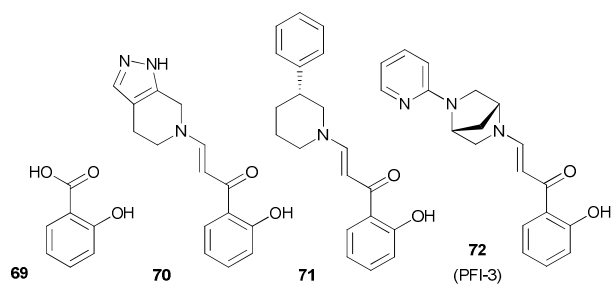


Fig 16 PB1 BD5 compounds (69-71) and PB1 BD5/SMARCA4 bromodomain inhibitor 72.

BRPF1

BRPF1 (Bromodomain and PHD Finger-containing 1) is a member of MOZ/MORF transcriptional coactivator complexes, which have been associated with oncology indications, particularly leukemia.⁶² Its bromodomain has proved very tractable to fragment optimisation as well as screening. For example, the dimethyl benzimidazolone **73** (Figure 17), closely related to the ATAD2 fragment hit **64** (Figure 13), was found in a BRD4 BD1 screen using ligand-observed STD-NMR, and was competitive with a known BET standard.⁶³ Analogue searches from results such as this helped to populate a screening set of lead-sized molecules, which was cross-screened against other bromodomains, including BRPF1 in a TR-FRET competition binding assay. BRPF1 specificity of the hits was confirmed by ¹⁵N HSQC NMR. Potent hits found directly from this screen included molecules that originated from fragment **73**. Compound **74** had good potency ($IC_{50} \sim 80$ nM), with significant selectivity by TR-FRET over BRPF2/3 ($> \sim 100$ -fold) and other bromodomains, critically BRD4 BD1 ($IC_{50} > 50$ μ M). It was also cell permeable in a NanoBRET assay measuring displacement of Halo-tagged histone H3.3 from NanoLuc-tagged BRPF1 bromodomain. As discussed in the conclusion section, crystal structures showed similar orientations of the benzimidazolone core of **73** and **74** in multiple bromodomains (Figure 20B).

Related compounds with similar properties have also been described by collaborators of the Structural Genomics Consortium (SGC). Researchers at Pfizer have reported the discovery of a potent, highly selective BRPF1-selective inhibitor PFI-4, believed to be related to **74**.⁶¹ A distinct sulfonamide-substituted benzimidazolone **75** has also been described in the context of the development of dual BRPF-TRIM24 bromodomain inhibitors.^{61,64} The compound is cell-permeable, with BRPF1 activity comparable to **74**, and 5-fold selectivity over BRPF2. Details of the discovery by this group of the sulfonamide-substituted benzimidazolones are unpublished, but as with the examples above its optimisation was assisted by the availability of numerous commercially available analogues.

The primary goal of chemical probe discovery is to establish a robust target-phenotype hypothesis. This can be strengthened by testing multiple structurally diverse chemical probes, to reduce the chance of confusing biology from off-target effects. A chemically distinct quinolinone inhibitor of the BRPF family, NI-57 (**76**) also originated from a bromodomain fragment screen.⁶⁵ It has recently been reported to bind to BRPF1, 2 and 3 with K_d of 31 nM, 108 nM and 408 nM respectively by ITC.⁶¹

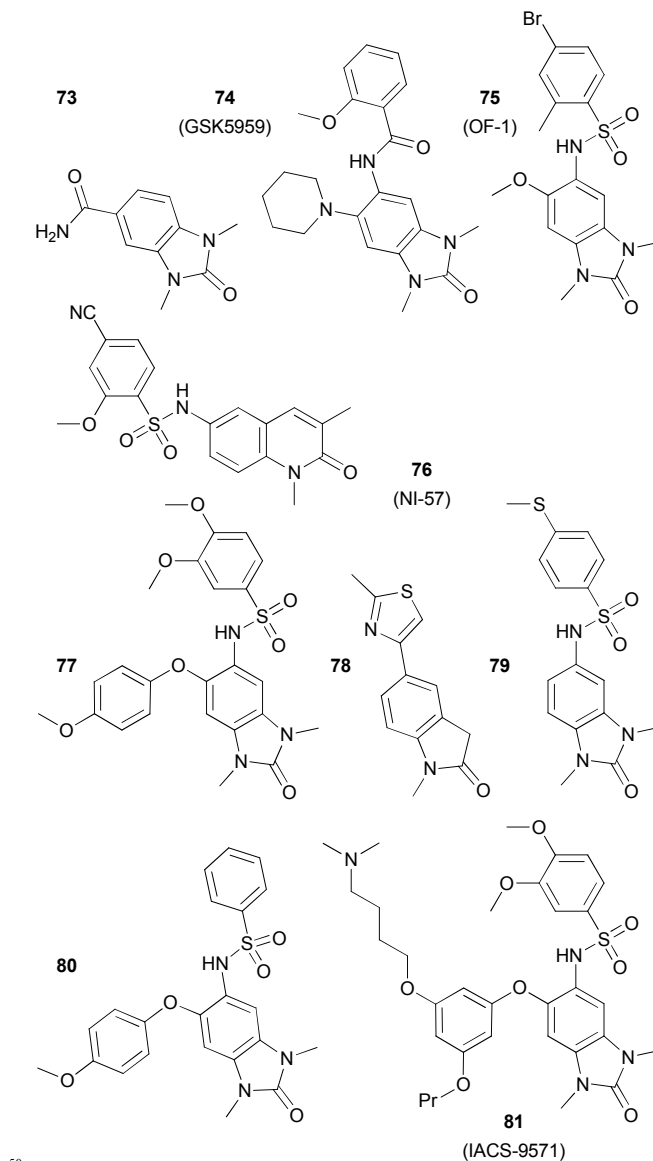


Fig. 17 BRPF and TRIM24 inhibitors 73-81.

TRIM24/TIF1 α

Very recently, analogues of the benzimidazolone BRPF1 inhibitors above have been shown to also inhibit the distantly related bromodomain of TRIM24 (Tripartite Motif containing protein 24). Knockdown of this gene, also known as TIF1 α (Transcription Intermediary Factor 1 α), has an antiproliferative effect in some cancer lines, for example breast cancer.⁶⁶

77 originated from an observation that substituted analogues of **75** were active in a TRIM24 AlphaScreen assay.⁶⁴ Further characterisation of **77**, the first published inhibitor of TIF1 α , showed that it binds potently (K_d 222 nM by ITC), with limited selectivity over BRPF1 (K_d 137 nM) and BRPF2 (K_d 1.1 μ M). This demonstrates again the potential for polypharmacology between bromodomains, even ones that are not closely related on the phylogenetic tree (Figure 2).

Another group has independently found similar dual TRIM24/BRPF compounds. Using a mixture of virtual screening,

targeted compound sets and diversity screening, **78** was identified as an efficient TRIM24 hit (AlphaScreen IC₅₀ 8.5 μM).⁶⁷ Its crystallographic binding mode suggested that replacing the thiazole group with sulfonamide derivatives may produce a vector targeting the “LAF/V” shelf (analogous to the WPF shelf of the BET proteins). Although unsuccessful in the original indolinone template, results from a replacement benzimidazolone template were more promising (e.g. **79**, TRIM24 IC₅₀ 4.9 μM). SAR from closely related high-throughput screening hits led to the investigation of benzimidazolone 5-substituents (**80**, IC₅₀ 1.5 μM, which showed an unexpected flipped binding mode in which the aryl ether rather than the aryl sulfonamide targets the LAF/V-shelf. In the TRIM24 complexes of **80** and the closely related **77**, the sulfonamide apparently contributes to binding by stacking against and positioning the ether substituent.^{64,67} Further elaboration targeting two additional regions, the “upper pocket” and the ZA channel, led to **81** (IACS-9571), a compound with improved potency (Kd 1.3nM), solubility (76 μM), and activity in a cellular target engagement assay. Although not especially selective over the BRPF bromodomains, its selectivity window over BRD4 is excellent (Kd > 10 μM). Together with pharmacokinetics suitable for *in vivo* dosing, this is the profile of a chemical probe useful for either the TRIM24 or the BRPF family bromodomains.

The examples of **77** and **81**, together with those in the BRPF1 section, illustrate the independent, convergent discovery by multiple investigators of closely related molecules sharing a common benzimidazolone template. This is perhaps not surprising, given the commercial availability of libraries of analogues and the shared knowledge underlying their selection. It is however encouraging that it has proved possible to modify the series with different substituents to produce different bromodomain binding profiles.

BRD9 and BRD7

The most recent bromodomains to be targeted using fragments are those of BRD9 and its close homologue BRD7. In one case study, pursuing analogues of a hit from a previous BRD4 BD1 screen, the purine **82** (Figure 18) was found to give positive thermal stabilisation of BRD4 BD1 and BRD9.⁶⁸ Analogues including phenyl 6-substituents were prepared, such as **83** and **84**, which were found to be more potent BRD9 inhibitors (e.g. Kd of 278 nM for **84**), with around five-fold selectivity over BRD4 BD1 *in vitro*. The compound was active in a NanoBRET assay measuring the displacement of tagged BRD9 bromodomain from Halo-histone H3.3 with IC₅₀ ~0.5 μM, and in this format no activity was found against BRD4. A crystal structure of **83** in BRD9 showed a bidentate hydrogen-bonding interaction with the conserved asparagine (N100) involving the purine N3 atom and the NH₂ group (Figure 19). The purine N9 atom makes the conserved hydrogen-bond with W1 of the water network. Compared to the previously determined BRD9 apo structure, in the complex with **83** some movement was observed in the sidechains of Phe44 and Phe47, leading to the suggestion that this more open pocket could provide opportunities for greater selectivity.

The optimisation of a separate series of 1-methylquinolones has recently been reported, starting from **56** (Figure 13), which

was first reported as an ATAD2 bromodomain fragment.⁵⁵ This was found to be an exceptionally ligand-efficient BRD9 inhibitor **60** (with reported Kd 5 μM, LE 0.60).⁶⁹ Using its ATAD2-bound structure as a model, the C7 position was chosen for elaboration to explore the BRD9 ZA channel. First, analogues incorporating various *N*-heterocyclic substituents were made and ranked according to their thermal stabilisation of BRD9, the valerolactam **85** being preferred. Synthesis of chiral analogues led to the discovery of **86** (BRD9 Kd 99 nM, LE 0.27). The (2*R*,3*S*) isomer was active, while its enantiomer showed no binding. Compound **86** inhibited IL6 production in LPS-stimulated THP-1 cells with IC₅₀ between 5-10 μM. No significant thermal stabilisation of 48 bromodomains tested was detected within the sensitivity limits of differential scanning

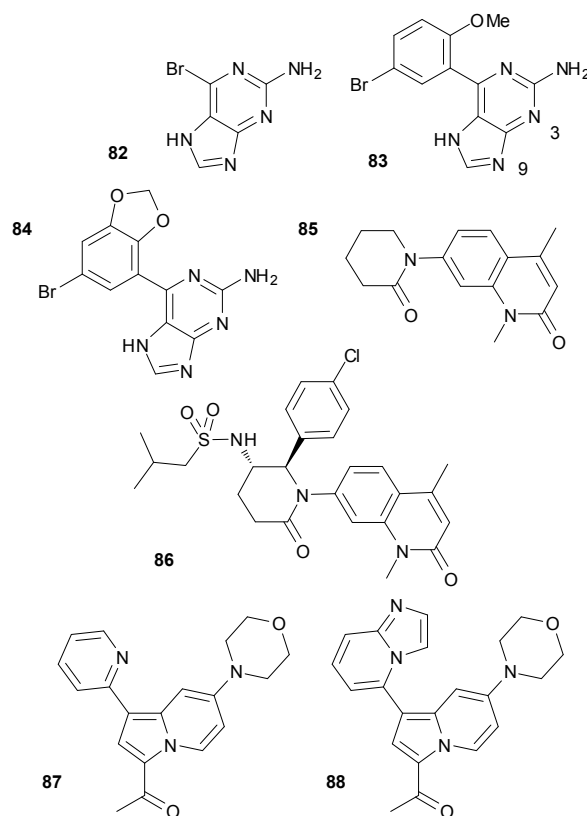


Fig. 18 BRD9 and BRD7 fragments and derived molecules **82-88**

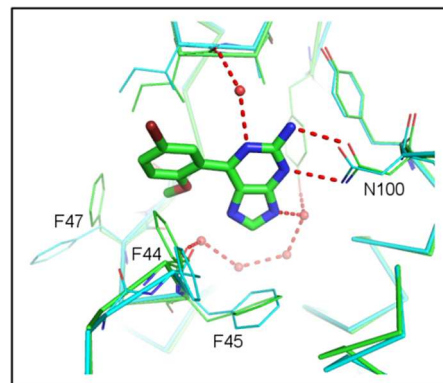


Fig. 19 Binding mode of **83** in BRD9 (green, PDB: 4xy8) overlaid with apo BRD9 structure (cyan, PDB: 3hme).

fluorimetry (DSF) apart from BRD9 and BRD7, suggesting that one of these targets may be responsible for the cellular activity. IL6 inhibition is highly sensitive to weak BET bromodomain inhibitors, and DSF only provides a qualitative measure of BET potency, but this result certainly justifies further investigation. Chemically distinct inhibitors of BRD9 and BRD7 with different bromodomain binding profiles, such as the recently reported I-BRD9 and BI-9564, might help to corroborate this mechanistic interpretation.^{61,70}

Most recently of all, the indolizine template first found to bind to BET bromodomains and optimised to inhibit BAZ2A/B (fragment **5** and compound **55**) has been adapted for BRD9. Analogues such as **87** were found active in a BRD9 AlphaScreen assay (IC₅₀ 500 nM) with around six-fold selectivity over BAZ2B. SAR-guided synthesis of analogues resulted in **88** (Kd by ITC of 68 nM for BRD9 and 368 nM for BRD7) with > 40-fold selectivity over BRD4 BD1 (Kd > 15 μM).⁷¹

Conclusion

Fragment screening is now firmly established as a means to discover ligand-efficient hits that compete for binding to the acetyl-lysine pockets of BET subfamily bromodomains. These are judged to be among the most tractable of this target class, as supported by a growing body of experimental data as well as by structure-based *in silico* calculations. Although current clinical compounds did not originate from fragment-based drug discovery, there are now several examples of fragment screening coupled with successful optimisation to give potent, ligand-efficient inhibitors selective for the BET bromodomains.

Other members of the family, while less well therapeutically validated, are still of interest. Chemical probes are needed to investigate their still poorly-understood functions. Reports of hits from fragment screening against these proteins have started to emerge. Encouragingly, for at least some members of the family it is possible to identify fragments with comparable ligand efficiencies to those that bind to BET. It now seems likely that KAc-mimetic fragments can be found for many if not all of the subset of bromodomains containing the typical conserved acetyl-lysine recognition elements. Examples of the optimisation of fragments into selective probe-quality molecules against several bromodomains are given above (e.g. CREBBP, BAZ2A/B,

BRPF1 and BRD7/9). Full details of the biological effects of these molecules have not yet emerged, so it is too early to say whether these compounds will achieve their goal of delivering novel, validated disease-relevant targets for drug discovery.

The KAc-site is by far the deepest cleft in the bromodomain fold. It is to this pocket that all reported bromodomain fragments bind. For practical reasons, target-based screening efforts (including fragment screens) have used isolated bromodomain modules. It is possible that additional functional allosteric binding sites could be present in the context of full-length bromodomain-containing proteins. However, no allosteric compounds have yet emerged from cell-based screens using intact proteins that first delivered BET bromodomain inhibitors.

Because of the conservation of the KAc-site between most bromodomains, it is not surprising that fragments such as some of those discussed above are able to bind to more than one member of the family. X-ray structures of **11** have been solved in the bromodomains of ATAD2, BRD2 BD1, CREBBP, PB1 and SMARCA4 (Figure 20A), besides the atypical PHIP BD2, to which it binds with a flipped mode. Compounds containing the 1,3-dimethyl benzimidazolone fragment such as **64**, **73** and **74** also adopt similar binding modes in multiple bromodomains (Figure 20B), as does acetaminophen (**9**, Figure 20C). This promiscuity brings advantages and disadvantages. Fragments may provide suitable starting points for optimisation against more than one target, enabling efficient parallel optimisation as well as serendipitous discoveries. Medicinal chemistry knowledge and SAR can be transferred between targets, and the construction of focused bromodomain family screening sets and arrays, which have featured heavily in several publications, is a realistic option for improving hit-rates. On the other hand, this conservation of sites and binding modes introduces the tricky issue of selectivity. Bromodomain KAc-site fragments require significant optimisation for selectivity as well as potency before they can be useful as chemical probes or, perhaps, as drugs. While strategies to optimise inhibitors for the BET family are known (growing into the WPF shelf, ZA channel, etc.), for other bromodomains such approaches are not generally so well understood.

This situation is reminiscent of the early days of protein kinase drug discovery. Similar fragments bind with high efficiency to the purine pockets of the ATP site of most kinases. This is one

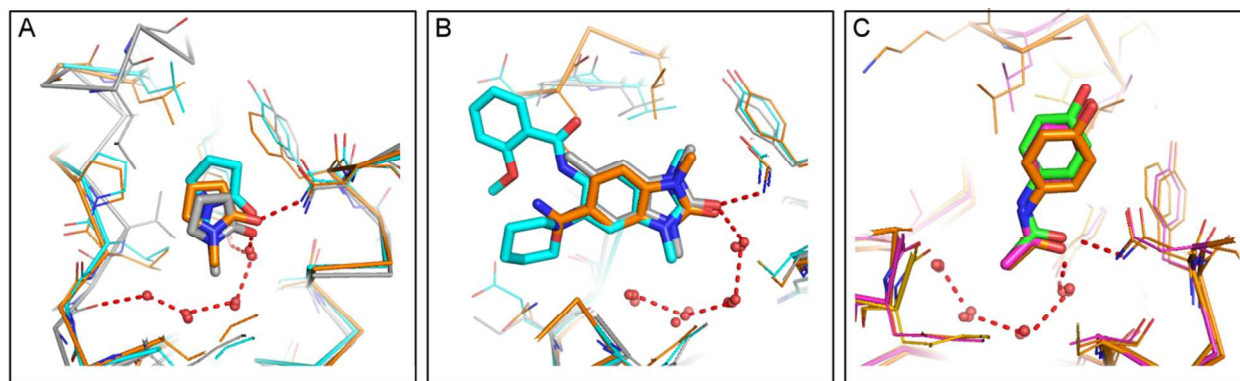


Fig. 20 Conserved binding modes of KAc-mimetic fragments bound into different superimposed bromodomains. A) **5** bound to BRD2 BD1 (grey, PDB: 4a9f), PB1 domain 5 (cyan, PDB: 3mb4) and SMARCA4 (orange, PDB: 3uvd). B) Benzimidazolone-containing fragments: **64** bound into ATAD2 (grey, PDB:4tyl), **73** bound into BRD4 BD1 (orange, PDB:4uyd), and **74** bound into BRPF1 (cyan, PDB: 4uye). C) **9** bound into BRD2 BD1 (orange, PDB: 4a9j), CREBBP (magenta, PDB: 4a9k) and BAZ2B (green, PDB: 4cut).

Cite this: DOI: 10.1039/c0xx00000x

www.rsc.org/xxxxxx

ARTICLE TYPE

major reason for their tractability: by growing into less conserved regions, potent and highly selective kinase inhibitors can be obtained. By analogy, the conserved KAc-site may be more of an opportunity than a liability for bromodomains, enabling target-class based lead discovery. By a curious coincidence, there are several examples of kinase inhibitors that also bind to BET-family bromodomains, despite the differences between the architectures of the purine and acetyl-lysine binding sites.^{59,72-74} These common activities may be more a consequence of the promiscuity of the BET proteins than any particular similarity between the pharmacophores of the kinase ATP site and the bromodomain KAc-site, because there are also examples of polypharmacology between BET bromodomains and other target classes, notably the gamma-aminobutyric acid receptor.⁷⁵ The high level of current research activity also resembles that seen within kinases, which might lead to parallel discoveries and novelty considerations as some of the referenced examples show.

Some authors have commented that experimental bromodomain fragment screening hit-rates seem to correlate with predicted ligandability, with targets containing shallow or polar active sites giving fewer confirmed hits. This has also been our experience. At this point, significant optimisation has only been reported in a limited number of cases. This may suggest that the difficulty of optimising fragments against some bromodomains should not be underestimated. In some cases, the region outside the KAc-site may simply be too shallow, polar or flexible to offer any chance to gain the necessary increase in potency while staying within drug-like chemical space.

Nevertheless, predictions of ligandability based on

interpretations of static bromodomain crystal structures may be misleading. Some fragments bind to ATAD2 and other bromodomains with unexpected displacement of some or all of the waters of the conserved network. Although the water network has been studied by molecular dynamics simulations,⁷⁶ the thermodynamic consequences of its partial or complete disruption remain poorly understood. In addition, the KAc-site environment is formed by the ZA and BC loop regions between α -helices, which have been seen to be mobile by solution NMR spectroscopy.^{45,77,78} Recently, similar ZA-loop flexibility has been reported in the structures of apo crystals of the ATAD2 bromodomain grown under different conditions.⁵⁶ The optimisation of selective CREBBP inhibitors was assisted by a pocket created by the movement of a flexible arginine sidechain, which was not visible in the unbound crystal structure (Figure 11A). In BRD9, sidechain movements result in adaptation to ligand-binding compared to the previously determined apo structure,⁶⁸ and larger-scale ZA loop movements can occur in response to relatively minor inhibitor modifications.⁷⁰ These results should caution against over-interpretation of rigid, unbound crystal structures for insights into bromodomain inhibitor binding. Whilst such movements may often be unpredictable, this flexibility is likely to create opportunities for ligands to bind to unexpected pockets, enabling potency and selectivity to be gained during fragment optimisation. In summary, although we now know much about the interactions of bromodomains with their ligands, further surprising discoveries should be expected.

Abbreviations

BD, Bromodomain; BET, Bromodomain and Extra Terminal FBDD, Fragment-Based Drug Discovery; GFP, Green Fluorescent Protein; ITC, Isothermal Titration Calorimetry; KAc, acetyl lysine; NMR, Nuclear Magnetic Resonance; SPR, Surface Plasmon Resonance.

Acknowledgements

Thanks to Ian Wall, Emmanuel Demont and Andrew Leach for their insightful comments during manuscript preparation.

Notes and references

⁷⁰ *Molecular Discovery Research, GlaxoSmithKline Medicines Research Centre, Gunnels Wood Road, Stevenage, Hertfordshire SG1 2NY, United Kingdom. Fax: +44 1438 763352; Tel: +44 1348 763246; E-mail: paul.a.bamborough@gsk.com*

References

- 1 E. Nicodeme, K. L. Jeffrey, U. Schaefer, S. Beinke, S. Dewell, C. W. Chung, R. Chandwani, I. Marazzi, P. Wilson, H. Coste, J. White, J. Kirilovsky, C. M. Rice, J. M. Lora, R. K. Prinjha, K. Lee and A. Tarakhovskiy. *Nature*, 2010, **468**, 1119. Suppression of inflammation by a synthetic histone mimic.
- 2 P. Filippakopoulos, J. Qi, S. Picaud, Y. Shen, W. B. Smith, O. Fedorov, E. M. Morse, T. Keates, T. T. Hickman, I. Felletar, M. Philpott, S. Munro, M. R. McKeown, Y. Wang, A. L. Christie, N. West, M. J. Cameron, B. Schwartz, T. D. Heightman, T. N. La, C. A. French, O. Wiest, A. L. Kung, S. Knapp and J. E. Bradner. *Nature*, 2010, **468**, 1067. Selective inhibition of BET bromodomains.
- 3 C. Chung, H. Coste, J. H. White, O. Mirguet, J. Wilde, R. L. Gosmini, C. Delves, S. M. Magny, R. Woodward, S. A. Hughes, E. V. Boursier, H. Flynn, A. M. Bouillot, P. Bamborough, J. M. Brusq, F. J. Gellibert, E. J. Jones, A. M. Riou, P. Homes, S. L. Martin, I. J. Uings, J. Toum, C. A. Clement, A. B. Boullay, R. L. Grimley, F. M. Blandel, R. K. Prinjha, K. Lee, J. Kirilovsky and E. Nicodeme. *J. Med. Chem.*, 2011, **54**, 3827. Discovery and Characterization of Small Molecule Inhibitors of the BET Family Bromodomains.
- 4 O. Mirguet, R. Gosmini, J. Toum, C. A. Clement, M. Barnathan, J. M. Brusq, J. E. Mordaunt, R. M. Grimes, M. Crowe, O. Pineau,

- M. Ajakane, A. Daugan, P. Jeffrey, L. Cutler, A. C. Haynes, N. N. Smithers, C. W. Chung, P. Bamborough, I. J. Uings, A. Lewis, J. Witherington, N. Parr, R. K. Prinjha and E. Nicodeme. *J. Med. Chem.*, 2013, **56**, 7501. Discovery of epigenetic regulator I-BET762: lead optimization to afford a clinical candidate inhibitor of the BET bromodomains.
- 5 R. Gosmini, V. L. Nguyen, J. Toum, C. Simon, J. M. Brusq, G. Krysa, O. Mirguet, A. M. Riou-Eymard, E. V. Boursier, L. Trottet, P. Bamborough, H. Clark, C. W. Chung, L. Cutler, E. H. Demont, R. Kaur, A. J. Lewis, M. B. Schilling, P. E. Soden, S. Taylor, A. L. Walker, M. D. Walker, R. K. Prinjha and E. Nicodeme. *J. Med. Chem.*, 2014, **57**, 8111. The discovery of I-BET726 (GSK1324726A), a potent tetrahydroquinoline ApoA1 up-regulator and selective BET bromodomain inhibitor.
- 10 K. G. McLure, E. M. Gesner, L. Tsujikawa, O. A. Kharenko, S. Attwell, E. Campeau, S. Wasiake, A. Stein, A. White, E. Fontano, R. K. Suto, N. C. Wong, G. S. Wagner, H. C. Hansen and P. R. Young. *PLOS ONE*, 2013, **8**, e83190. RVX-208, an inducer of ApoA-I in humans, is a BET bromodomain antagonist.
- 15 6 M. Brand, A. M. Measures, B. G. Wilson, W. A. Cortopassi, R. Alexander, M. Hoss, D. S. Hewings, T. P. Rooney, R. S. Paton and S. J. Conway. *ACS Chem. Biol.*, 2015, **10**, 22. Small Molecule Inhibitors of Bromodomain-Acetyl-lysine Interactions.
- 20 8 D. Gallenkamp, K. A. Gelato, B. Haendler and H. Weinmann. *ChemMedChem.*, 2014, **9**, 438. Bromodomains and their pharmacological inhibitors.
- 25 9 C. Chung and D. F. Tough. *Drug Discovery Today: Therapeutic Strategies*, 2012, **9**, e111-e120. Bromodomains: a new target class for small molecule drug discovery.
- 30 10 R. K. Prinjha, J. Witherington and K. Lee. *Trends Pharmacol. Sci.*, 2012, **33**, 146. Place your BETs: the therapeutic potential of bromodomains.
- 11 R. Sanchez, J. Meslamani and M. M. Zhou. *Biochim. Biophys. Acta*, 2014, **1839**, 676. The bromodomain: from epigenome reader to druggable target.
- 35 12 P. Filippakopoulos and S. Knapp. *FEBS Lett.*, 2012, **586**, 2692. The bromodomain interaction module.
- 13 L. R. Vidler, N. Brown, S. Knapp and S. Hoelder. *J. Med. Chem.*, 2012, **55**, 7346. Druggability analysis and structural classification of bromodomain acetyl-lysine binding sites.
- 40 14 S. B. Shuker, P. J. Hajduk, R. P. Meadows and S. W. Fesik. *Science*, 1996, **274**, 1531. Discovering high-affinity ligands for proteins: SAR by NMR.
- 15 M. Congreve, G. Chessari, D. Tisi and A. J. Woodhead. *J. Med. Chem.*, 2008, **51**, 3661. Recent developments in fragment-based drug discovery.
- 45 16 D. A. Erlanson, R. S. McDowell and T. O'Brien. *J. Med. Chem.*, 2004, **47**, 3463. Fragment-based drug discovery.
- 17 G. E. De Kloe, D. Bailey, R. Leurs and I. J. de Esch. *Drug Discov. Today*, 2009, **14**, 630. Transforming fragments into candidates: small becomes big in medicinal chemistry.
- 50 18 J. Fejzo, C. A. Lepre, J. W. Peng, G. W. Bemis, Ajay, M. A. Murcko and J. M. Moore. *Chem. Biol.*, 1999, **6**, 755. The SHAPES strategy: an NMR-based approach for lead generation in drug discovery.
- 55 19 M. M. Hann, A. R. Leach and G. Harper. *J. Chem. Inf. Comput. Sci.*, 2001, **41**, 856. Molecular complexity and its impact on the probability of finding leads for drug discovery.
- 20 M. Congreve, R. Carr, C. Murray and H. Jhoti. *Drug Discov. Today*, 2003, **8**, 876. A 'rule of three' for fragment-based lead discovery?
- 21 H. Jhoti, G. Williams, D. C. Rees and C. W. Murray. *Nat. Rev. Drug Discov.*, 2013, **12**, 644. The 'rule of three' for fragment-based drug discovery: where are we now?
- 22 P. Filippakopoulos, S. Picaud, M. Mangos, T. Keates, J. P. Lambert, D. Barsyte-Lovejoy, I. Felletar, R. Volkmer, S. Muller, T. Pawson, A. C. Gingras, C. H. Arrowsmith and S. Knapp. *Cell*, 2012, **149**, 214. Histone recognition and large-scale structural analysis of the human bromodomain family.
- 23 A. L. Hopkins, G. M. Keseru, P. D. Leeson, D. C. Rees and C. H. Reynolds. *Nat. Rev. Drug Discov.*, 2014, **13**, 105. The role of ligand efficiency metrics in drug discovery.
- 24 X. Lucas, D. Wohlwend, M. Hugle, K. Schmidt-kunz, S. Gerhardt, R. Schule, M. Jung, O. Einsle and S. Gunther. *Angew. Chem. Int. Ed Engl.*, 2013, **52**, 14055. 4-Acyl pyrroles: mimicking acetylated lysines in histone code reading.
- 25 L. R. Vidler, P. Filippakopoulos, O. Fedorov, S. Picaud, S. Martin, M. Tomsett, H. Woodward, N. Brown, S. Knapp and S. Hoelder. *J. Med. Chem.*, 2013, **56**, 8073. Discovery of Novel Small-Molecule Inhibitors of BRD4 Using Structure-Based Virtual Screening.
- 26 C.-W. Chung, A. W. Dean, J. M. Woolven and P. Bamborough. *J. Med. Chem.*, 2012, **55**, 576. Fragment-based discovery of bromodomain inhibitors part 1: inhibitor binding modes and implications for lead discovery.
- 27 P. Bamborough, H. Diallo, J. D. Goodacre, L. Gordon, A. Lewis, J. T. Seal, D. M. Wilson, M. D. Woodrow and C. W. Chung. *J. Med. Chem.*, 2012, **55**, 587. Fragment-based discovery of bromodomain inhibitors part 2: optimization of phenylisoxazole sulfonamides.
- 28 N. K. Mishra, A. K. Urlick, S. W. Ember, E. Schonbrunn and W. C. Pomerantz. *ACS Chem. Biol.*, 2014, **9**, 2755. Fluorinated Aromatic Amino Acids Are Sensitive F NMR Probes for Bromodomain-Ligand Interactions.
- 29 BAZ2B PDB structures: entries 4cut, 4cuq, 4cur, 4cus, 4cup. A.R. Bradley, Y. Liu, T. Krojer, C. Bountra, C.H. Arrowsmith, A. Edwards, S. Knapp, F. von Delft. Downloaded from <http://www.rcsb.org> on 15th June 2015.
- 30 Sachchidanand, L. Resnick-Silverman, S. Yan, S. Mutjaba, W. J. Liu, L. Zeng, J. J. Manfredi and M. M. Zhou. *Chem. Biol.*, 2006, **13**, 81. Target structure-based discovery of small molecules that block human p53 and CREB binding protein association.
- 31 O. Mirguet, Y. Lamotte, F. Donche, J. Toum, F. Gellibert, A. Bouillot, R. Gosmini, V. L. Nguyen, D. Delannee, J. Seal, F. Blandel, A. B. Boullay, E. Boursier, S. Martin, J. M. Brusq, G. Krysa, A. Riou, R. Tellier, A. Costaz, P. Huet, Y. Dudit, L. Trottet, J. Kirilovsky and E. Nicodeme. *Bioorg. Med. Chem. Lett.*, 2012, **22**, 2963. From ApoA1 upregulation to BET family bromodomain inhibition: discovery of I-BET151.
- 32 J. Seal, Y. Lamotte, F. Donche, A. Bouillot, O. Mirguet, F. Gellibert, E. Nicodeme, G. Krysa, J. Kirilovsky, S. Beinke, S.

- McCleary, I. Rioja, P. Bamborough, C. W. Chung, L. Gordon, T. Lewis, A. L. Walker, L. Cutler, D. Lugo, D. M. Wilson, J. Witherington, K. Lee and R. K. Prinjha. *Bioorg. Med. Chem. Lett.*, 2012, **22**, 2968. Identification of a novel series of BET family bromodomain inhibitors: binding mode and profile of I-BET151 (GSK1210151A).
- 33 M. Philpott, J. Yang, T. Tumber, O. Fedorov, S. Uttarkar, P. Filippakopoulos, S. Picaud, T. Keates, I. Felletar, A. Ciulli, S. Knapp and T. D. Heightman. *Mol. Biosyst.*, 2011, **7**, 2899. Bromodomain-peptide displacement assays for interactome mapping and inhibitor discovery.
- 34 D. S. Hewings, M. Wang, M. Philpott, O. Fedorov, S. Uttarkar, P. Filippakopoulos, S. Picaud, C. Vuppusetty, B. Marsden, S. Knapp, S. J. Conway and T. D. Heightman. *J. Med. Chem.*, 2011, **54**, 6761. 3,5-dimethylisoxazoles act as acetyl-lysine-mimetic bromodomain ligands.
- 35 D. Hay, O. Fedorov, P. Filippakopoulos, S. Martin, M. Philpott, S. Picaud, D. S. Hewings, S. Uttarkar, T. D. Heightman and S. J. Conway. *MedChemComm*, 2013, **4**, 140. The design and synthesis of 5- and 6-isoxazolylbenzimidazoles as selective inhibitors of the BET bromodomains.
- 36 V. S. Gehling, M. C. Hewitt, R. G. Vaswani, Y. Leblanc, A. Cote, C. G. Nasveschuk, A. M. Taylor, J. C. Harmange, J. E. Audia, E. Pardo, S. Joshi, P. Sandy, J. A. Mertz, R. J. Sims, III, L. Bergeron, B. M. Bryant, S. Bellon, F. Poy, H. Jayaram, R. Sankaranarayanan, S. Yellapantula, S. N. Bangalore, S. Birudukota and B. K. Albrecht. *ACS Med. Chem. Lett.*, 2013, **4**, 835. Discovery, Design, and Optimization of Isoxazole Azepine BET Inhibitors.
- 37 P. P. Sharp, J.-M. Garnier, D. C. S. Huang and C. J. Burns. *MedChemComm*, 2014, **5**, 1834. Evaluation of functional groups as acetyl-lysine mimetics for BET bromodomain inhibition.
- 38 P. V. Fish, P. Filippakopoulos, G. Bish, P. E. Brennan, M. E. Bunnage, A. S. Cook, O. Fedorov, B. S. Gerstenberger, H. Jones, S. Knapp, B. Marsden, K. Nocka, D. R. Owen, M. Philpott, S. Picaud, M. J. Primiano, M. J. Ralph, N. Sciammetta and J. D. Trzuppek. *J. Med. Chem.*, 2012, **55**, 9831. Identification of a chemical probe for bromo and extra C-terminal bromodomain inhibition through optimization of a fragment-derived hit.
- 39 J. Wu, J. Shin, C. M. M. Williams, K. F. Geoghegan, S. W. Wright, D. C. Limburg, P. Sahasrabudhe, P. D. Bonin, B. A. Lefker and S. Ramsey. *MedChemComm*, 2014, **5**, 1871. Design and chemoproteomic functional characterization of a chemical probe targeted to bromodomains of BET family proteins.
- 40 V. L. Nienaber, P. L. Richardson, V. Klighofer, J. J. Bouska, V. L. Giranda and J. Greer. *Nat. Biotechnol.*, 2000, **18**, 1105. Discovering novel ligands for macromolecules using X-ray crystallographic screening.
- 41 M. J. Hartshorn, C. W. Murray, A. Cleasby, M. Frederickson, I. J. Tickle and H. Jhoti. *J. Med. Chem.*, 2005, **48**, 403. Fragment-based lead discovery using X-ray crystallography.
- 42 G. Lolli and R. Battistutta. *Acta Crystallogr. D Biol. Crystallogr.*, 2013, **69**, 2161. Different orientations of low-molecular-weight fragments in the binding pocket of a BRD4 bromodomain.
- 43 L. Zhao, D. Cao, T. Chen, Y. Wang, Z. Miao, Y. Xu, W. Chen, X. Wang, Y. Li, Z. Du, B. Xiong, J. Li, C. Xu, N. Zhang, J. He and J. Shen. *J. Med. Chem.*, 2013, **56**, 3833. Fragment-based drug discovery of 2-thiazolidinones as inhibitors of the histone reader BRD4 bromodomain.
- 44 L. Zhao, Y. Wang, D. Cao, T. Chen, Q. Wang, Y. Li, Y. Xu, X. Wang, D. Chen, L. Chen, Y. Chen, G. Xia, Z. Shi, Y. Liu, Y. Lin, Z. Miao, J. Shen and B. Xiong. *J. Med. Chem.*, 2015, **58**, 1281. Fragment-Based Drug Discovery of 2-Thiazolidinones as BRD4 inhibitors: 2. Structure-based Optimization.
- 45 C. Dhalluin, J. E. Carlson, L. Zeng, C. He, A. K. Aggarwal and M. M. Zhou. *Nature*, 1999, **399**, 491. Structure and ligand of a histone acetyltransferase bromodomain.
- 46 L. Zeng, J. Li, M. Muller, S. Yan, S. Mujtaba, C. Pan, Z. Wang and M. M. Zhou. *J. Am. Chem. Soc.*, 2005, **127**, 2376. Selective small molecules blocking HIV-1 Tat and coactivator PCAF association.
- 47 C. Pan, M. Mezei, S. Mujtaba, M. Muller, L. Zeng, J. Li, Z. Wang and M. M. Zhou. *J. Med. Chem.*, 2007, **50**, 2285. Structure-guided optimization of small molecules inhibiting human immunodeficiency virus 1 Tat association with the human coactivator p300/CREB binding protein-associated factor.
- 48 Q. Wang, R. Wang, B. Zhang, S. Zhang, Y. Zheng and Z. Wang. *MedChemComm*, 2013, **4**, 737. Small organic molecules targeting PCAF bromodomain as potent inhibitors of HIV-1 replication.
- 49 T. P. Rooney, P. Filippakopoulos, O. Fedorov, S. Picaud, W. A. Cortopassi, D. A. Hay, S. Martin, A. Tumber, C. M. Rogers, M. Philpott, M. Wang, A. L. Thompson, T. D. Heightman, D. C. Pryde, A. Cook, R. S. Paton, S. Muller, S. Knapp, P. E. Brennan and S. J. Conway. *Angew. Chem. Int. Ed Engl.*, 2014, **53**, 6126. A series of potent CREBBP bromodomain ligands reveals an induced-fit pocket stabilized by a cation- π interaction.
- 50 D. A. Hay, O. Fedorov, S. Martin, D. C. Singleton, C. Tallant, C. Wells, S. Picaud, M. Philpott, O. P. Monteiro, C. M. Rogers, S. J. Conway, T. P. Rooney, A. Tumber, C. Yapp, P. Filippakopoulos, M. E. Bunnage, S. Muller, S. Knapp, C. J. Schofield and P. E. Brennan. *J. Am. Chem. Soc.*, 2014, **136**, 9308. Discovery and optimization of small-molecule ligands for the CBP/p300 bromodomains.
- 51 F. M. Ferguson, O. Fedorov, A. Chaikuad, M. Philpott, J. Muniz, I. Felletar, D. F. von, T. D. Heightman, S. Knapp, C. Abell and A. Ciulli. *J. Med. Chem.*, 2013, **56**, 10183. Targeting low-druggability bromodomains: Fragment based screening and inhibitor design against the BAZ2B bromodomain.
- 52 P. Chen, A. Chaikuad, P. Bamborough, M. Bantscheff, C. Bountra, C. W. Chung, O. Fedorov, P. Grandi, D. Jung, R. Lesniak, M. Lindon, S. Muller, M. Philpott, R. Prinjha, C. Rogers, C. Selenski, C. Tallant, T. Werner, T. M. Willson, S. Knapp and D. H. Drewry. *J. Med. Chem. in press.*, 2015, **DOI: 10.1021/acs.jmedchem.5b00209**. Discovery and Characterization of GSK2801, a Selective Chemical Probe for the Bromodomains BAZ2A and BAZ2B.
- 53 L. Drouin, S. McGrath, L. R. Vidler, A. Chaikuad, O. Monteiro, C. Tallant, M. Philpott, C. Rogers, O. Fedorov, M. Liu, W. Akhtar, A. Hayes, F. Raynaud, S. Muller, S. Knapp and S. Hoelder. *J. Med. Chem.*, 2015, **58**, 2553. Structure Enabled

- Design of BAZ2-ICR, A Chemical Probe Targeting the Bromodomains of BAZ2A and BAZ2B.
- 54 E. V. Kalashnikova, A. S. Revenko, A. T. Gemo, N. P. Andrews, C. G. Tepper, J. X. Zou, R. D. Cardiff, A. D. Borowsky and H. W. Chen. *Cancer Res.*, 2010, **70**, 9402. ANCCA/ATAD2 overexpression identifies breast cancer patients with poor prognosis, acting to drive proliferation and survival of triple-negative cells through control of B-Myb and EZH2.
- 55 A. Chaikvad, A. M. Petros, O. Federov, J. Xu and S. Knapp. *MedChemComm*, 2014, **5**, 1843. Structure-based approaches towards identification of fragments for the low-druggability ATAD2 bromodomain.
- 56 G. Poncet-Montange, Y. Zhan, J. P. Bardenhagen, A. Petrocchi, E. Leo, X. Shi, G. R. Lee, P. G. Leonard, M. K. Geck Do, M. G. Cardozo, J. N. Andersen, W. S. Palmer, P. Jones and J. E. Ladbury. *Biochem. J.*, 2015, **466**, 337. Observed bromodomain flexibility reveals histone peptide- and small molecule ligand-compatible forms of ATAD2.
- 57 E. H. Demont, C. Chung, R. Furze, P. Grandi, A. M. Michon, C. Wellaway, N. Barrett, A. Bridges, P. D. Craggs, H. Diallo, D. J. Dixon, C. Douault, A. Emmons, E. J. Jones, B. Karamshi, K. Locke, D. J. Mitchell, B. Mouzon, R. K. Prinjha, A. D. Roberts, R. J. Sheppard, R. J. Watson and P. Bamborough. *J. Med. Chem. in press.*, 2015, **DOI: to be confirmed**. Fragment-based discovery of low-micromolar ATAD2 bromodomain inhibitors.
- 58 M. J. Harner, B. A. Chauder, J. Phan and S. W. Fesik. *J. Med. Chem.*, 2014, **57**, 9687. Fragment-Based Screening of the Bromodomain of ATAD2.
- 59 S. W. Ember, J. Y. Zhu, S. H. Olesen, M. P. Martin, A. Becker, N. Berndt, G. I. Georg and E. Schonbrunn. *ACS Chem. Biol.*, 2014, **9**, 1160. Acetyl-lysine binding site of bromodomain-containing protein 4 (BRD4) interacts with diverse kinase inhibitors.
- 60 P. B. B. PDB structures: entries 4y03, 4q0n and 4q0o. P. Filippakopoulos, S. Picaud, I. Felletar, O. Federov, S. Martin, O. Monteiro, A. Chaikvad, W. Yue, F. von Delft, A. M. Edwards, C. H. Arrowsmith, C. Bountra, S. Knapp. Downloaded from <http://www.rcsb.org> on 15th June.
- 61 The Structural Genomics Consortium chemical probes website, <http://www.thesgc.org/chemical-probes/epigenetics>, accessed June 15th 2015.
- 62 S. Carlson and K. C. Glass. *J. Cell Physiol*, 2014, **229**, 1571. The MOZ histone acetyltransferase in epigenetic signaling and disease.
- 63 E. H. Demont, P. Bamborough, C. W. Chung, P. D. Craggs, D. Fallon, L. J. Gordon, P. Grandi, C. I. Hobbs, J. Hussain, E. J. Jones, G. A. Le, A. M. Michon, D. J. Mitchell, R. K. Prinjha, A. D. Roberts, R. J. Sheppard and R. J. Watson. *ACS Med. Chem. Lett.*, 2014, **5**, 1190. 1,3-Dimethyl Benzimidazolones Are Potent, Selective Inhibitors of the BRPF1 Bromodomain.
- 64 J. M. Bennett, O. Federov, C. Tallant, O. P. Monteiro, J. Meier, V. Gamble, P. Savitski, G. A. Nunez-Alonso, B. Haendler, C. Rogers, P. E. Brennan, S. Muller and S. Knapp. *J. Med. Chem. in press.*, 2015, **DOI: 10.1021/acs.jmedchem.5b00458**. Discovery of a Chemical Tool Inhibitor Targeting the Bromodomains of TRIM24 and BRPF.
- 65 Chemical probes for the bromodomain of the BRPF family. Fish, P.V. Presented at the 4th Oxford Symposium of Epigenetic Mechanisms in Health and Disease, Oxford, June, 2015.
- 66 W. W. Tsai, Z. Wang, T. T. Yiu, K. C. Akdemir, W. Xia, S. Winter, C. Y. Tsai, X. Shi, D. Schwarzer, W. Plunkett, B. Aronow, O. Gozani, W. Fischle, M. C. Hung, D. J. Patel and M. C. Barton. *Nature*, 2010, **468**, 927. TRIM24 links a non-canonical histone signature to breast cancer.
- 67 W. S. Palmer, G. Poncet-Montange, G. Liu, A. Petrocchi, N. Reyna, G. Subramanian, J. Theroff, A. Yau, M. Kost-Alimova, J. P. Bardenhagen, E. Leo, H. E. Sheppard, T. N. Tieu, X. Shi, Y. Zhan, S. Zhao, G. Draetta, C. Toniatti, P. Jones, M. K. Geck Do and J. N. Andersen. *J. Med. Chem. in press.*, 2015, **DOI: 10.1021/acs.jmedchem.5b00405**. Structure-guided design of IACS-9571, a selective high-affinity dual TRIM24-BRPF1 bromodomain inhibitor.
- 68 S. Picaud, M. Strocchia, S. Terracciano, G. Lauro, J. Mendez, D. L. Daniels, R. Riccio, G. Bifulco, I. Bruno and P. Filippakopoulos. *J. Med. Chem.*, 2015, **58**, 2718. 9H-Purine Scaffold Reveals Induced-Fit Pocket Plasticity of the BRD9 Bromodomain.
- 69 P. G. Clark, L. C. Vieira, C. Tallant, O. Federov, D. C. Singleton, C. M. Rogers, O. P. Monteiro, J. M. Bennett, R. Baronio, S. Muller, D. L. Daniels, J. Mendez, S. Knapp, P. E. Brennan and D. J. Dixon. *Angew. Chem. Int. Ed.*, 2015, **54**, 6217. LP99: Discovery and Synthesis of the First Selective BRD7/9 Bromodomain Inhibitor.
- 70 N. H. Theodoulou, P. Bamborough, A. J. Bannister, I. Becher, R. A. Bit, K. H. Che, C. W. Chung, A. Dittmann, G. Drewes, D. H. Drewry, L. Gordon, P. Grandi, M. Leveridge, M. Lindon, A. M. Michon, J. Molnar, S. C. Robson, N. C. Tomkinson, T. Kouzarides, R. K. Prinjha and P. G. Humphreys. *J. Med. Chem. in press*, 2015, **DOI:10.1021/acs.jmedchem.5b00256**. The Discovery of I-BRD9, a Selective Cell Active Chemical Probe for Bromodomain Containing Protein 9 Inhibition.
- 71 D. A. Hay, C. Rogers, O. Federov, C. Tallant, S. Martin, O. Monteiro, S. Muller, S. Knapp, C. J. Schofield and P. E. Brennan. *MedChemComm in press.*, 2015, **DOI:10.1039/c5md00152h**. Design and synthesis of potent and selective inhibitors of BRD7 and BRD9 bromodomains.
- 72 M. P. Martin, S. H. Olesen, G. I. Georg and E. Schonbrunn. *ACS Chem. Biol.*, 2013, **8**, 2360. Cyclin-dependent kinase inhibitor dinaciclib interacts with the acetyl-lysine recognition site of bromodomains.
- 73 A. Dittmann, T. Werner, C. W. Chung, M. M. Savitski, S. M. Falth, P. Grandi, C. Hopf, M. Lindon, G. Neubauer, R. K. Prinjha, M. Bantscheff and G. Drewes. *ACS Chem. Biol.*, 2014, **9**, 495. The commonly used PI3-kinase probe LY294002 is an inhibitor of BET bromodomains.
- 74 P. Ciceri, S. Muller, A. O'Mahony, O. Federov, P. Filippakopoulos, J. P. Hunt, E. A. Lasater, G. Pallares, S. Picaud, C. Wells, S. Martin, L. M. Wodicka, N. P. Shah, D. K. Treiber and S. Knapp. *Nat. Chem. Biol.*, 2014, **10**, 305. Dual kinase-bromodomain inhibitors for rationally designed polypharmacology.

-
- 75 P. Filippakopoulos, S. Picaud, O. Fedorov, M. Keller, M. Wrobel, O. Morgenstern, F. Bracher and S. Knapp. *Bioorg. Med. Chem.*, 2012, **20**, 1878. Benzodiazepines and benzotriazepines as protein interaction inhibitors targeting bromodomains of the BET family.
- 76 D. Huang, E. Rossini, S. Steiner and A. Caflisch. *ChemMedChem.*, 2014, **9**, 573. Structured water molecules in the binding site of bromodomains can be displaced by cosolvent.
- 77 S. Mujtaba, L. Zeng and M. M. Zhou. *Oncogene*, 2007, **26**, 5521. Structure and acetyl-lysine recognition of the bromodomain.
- 78 L. Zeng, Q. Zhang, G. Gerona-Navarro, N. Moshkina and M. M. Zhou. *Structure.*, 2008, **16**, 643. Structural basis of site-specific histone recognition by the bromodomains of human coactivators PCAF and CBP/p300.

15